

Equivalent beams for carbon nanotubes

P. Papanikos^{a,*}, D.D. Nikolopoulos^a, K.I. Tserpes^b

^a Department of Product and Systems Design Engineering, University of the Aegean, Ermoupolis, Syros 84100, Greece

^b Laboratory of Technology and Strength of Materials, Department of Mechanical Engineering and Aeronautics, University of Patras, Patras 26500, Greece

Received 26 September 2007; received in revised form 27 November 2007; accepted 7 December 2007

Available online 4 March 2008

Abstract

Atomistic-based FE analysis is combined with mechanics of materials to evaluate the geometrical characteristics and elastic properties of beams that possess the same tensile, bending and torsional behavior with carbon nanotubes (CNTs). Using 3D FE analysis and assuming a linear behavior of the C–C bonds, the tensile, bending and torsional rigidities of CNTs are initially derived. Then, for the selected beam, the equivalent dimensions, geometrical constants and elastic moduli are evaluated. Both solid and hollow cylindrical beams are considered. Relations between the equivalent properties and chiral index are obtained for armchair and zigzag nanotubes, thus providing a direct evaluation of the equivalent beam for any CNT of those two types. The comparison between the solid and hollow cylinders shows that the latter is more suitable for use as equivalent beam because its dimensions are much closer to the actual dimensions of the nanotube. The obtained elastic moduli of the equivalent hollow cylinder compare very well with relative results published in the literature.

© 2007 Elsevier B.V. All rights reserved.

PACS: 61.46.De; 62.25.–g; 02.70.Dh; 34.20.–b

Keywords: Carbon nanotubes; Finite element analysis; Beams

1. Introduction

Towards the establishment of carbon nanotubes (CNTs) as prospective mechanical reinforcements of polymers, two fundamental issues must be fully addressed: the effective interfacial load transfer between the nanotube and the matrix and the evaluation of the bulk mechanical properties as a function of specific parameters concerning the nanotube structure (geometry and defects) and manufacturing process (dispersion and alignment). Currently, both issues are being investigated thoroughly using experimental techniques and theoretical models. However, due to the difficulties of experimentation at the nanoscale, theoretical modeling is more attractive.

During the first years of theoretical investigation of CNTs, atomistic approaches were solely used. However,

in the last few years, due to the large computational effort required by atomistic approaches, they are progressively replaced by continuum approaches. The continuum approaches used so far may be classified into three categories: the atomistic-based continuum approaches, the analytical/micromechanical approaches and the numerical approaches.

In the first category belong the approaches that draw data from atomistic methods, such as molecular dynamics and force-fields, for the behavior of CNTs and the interfacial load transfer between the nanotube and the matrix, and assign them in a representative unit cell whose elastic properties are evaluated using continuum methods. For example, [1] modeled the nanotube, the local polymer near the nanotube and the nanotube/polymer interface as an effective continuum fiber by using an equivalent-continuum model. The effective fiber retains the local molecular structure and bonding information, as defined by molecular dynamics, and serves as a means for linking the

* Corresponding author. Tel.: +30 2281097000; fax: +30 2281097109.
E-mail address: ppap@syros.aegean.gr (P. Papanikos).

equivalent-continuum and micromechanics models. The micromechanics method is then available for the prediction of bulk mechanical properties of single-walled CNT/polymer composites. The main drawback of the atomistic-based continuum approaches is that they involve very complicated analyses and huge computational efforts imposed by the incorporated atomistic method.

In the second category belong the analytical and micromechanical models well established in fiber-reinforced composites. These approaches have been mainly used for modeling the interfacial load transfer between the nanotube and the matrix. Exception is the work of [2] who obtained the effective elastic properties of CNT-reinforced composites through a variety of micromechanical techniques. Although the analytical/micromechanical approaches provide detailed information about the interaction between the nanotube and the matrix, they are locally oriented, thus being inapplicable in larger scale systems such as nanocomposite specimens.

Contrary to the previous two approaches, for which a considerable number of works have been published, the use of numerical approaches is restricted to the use of the FE method either as supporting method to obtain necessary data [3] or as verification method [2,4]. Only the works of [5,6] solved representative volume elements using the FE method in order to evaluate the effective elastic properties of CNT-reinforced composites.

From the above it is concluded that there is still a demand for developing modeling techniques able to efficiently simulate the behavior of CNT-reinforced composites. To the authors' opinion, the ongoing research on this issue must focus on the modification of the existed continuum methods in order to accurately capture the behavior of CNTs. Towards this goal, the present paper aims to contribute by evaluating the equivalent properties of beams being suitable for simulating the behavior of CNTs embedded in elastic medium using the FE method.

2. The equivalent beam

The concept of the 'equivalent beam' is based on the condition of identical mechanical behavior between the CNT and the beam, which corresponds to identical tensile, bending and torsional behaviors. As for elastic beams, these behaviors are designated by the corresponding rigidities and in order to fully define the equivalent beam, it suffices to evaluate its equivalent properties (geometrical characteristics and elastic properties) from the nanotube's rigidities.

2.1. FE analysis of CNTs: derivation of rigidities

In order to derive the nanotube's rigidities, the 3D FE model proposed by [7] is used. The model treats CNTs as space-frame structures. Using 3D elastic beam elements, the exact atomic structure of the nanotubes is modeled. The elastic moduli of the beam elements are determined

using a linkage between molecular and continuum mechanics proposed by [8]. The following relationships between the structural mechanics parameters and the molecular mechanics parameters are obtained:

$$\frac{E_b A_b}{\ell} = k_r, \quad \frac{E_b I_b}{\ell} = k_\theta, \quad \frac{G_b J_b}{\ell} = k_\tau \quad (1)$$

Here, ℓ is the bond length equal to 0.1421 nm; E_b and G_b are the bond's Young's modulus and shear modulus, respectively; I_b and J_b are the moment of inertia and polar moment of inertia, respectively, and k_r , k_θ , and k_τ are the bond stretching, bond bending and torsional resistance force constants, respectively. Assuming a solid circular cross-sectional area of the beams with diameter d and setting $A_b = \frac{\pi d^2}{4}$, $I_b = \frac{\pi d^4}{64}$ and $J_b = \frac{\pi d^4}{32}$, Eq. (1) give

$$d = 4\sqrt{\frac{k_\theta}{k_r}}, \quad E_b = \frac{k_r^2 \ell}{4\pi k_\theta}, \quad G_b = \frac{k_r^2 k_\tau \ell}{8\pi k_\theta^2} \quad (2)$$

Eq. (2) give all necessary input parameters for the beam elements. In the present study, the following values were used for the force constants [9,10]

$$k_r = 938 \text{ kcal mole}^{-1} \text{ \AA}^{-2} = 6.52 \times 10^{-7} \text{ N/nm}$$

$$k_\theta = 126 \text{ kcal mole}^{-1} \text{ rad}^{-2} = 8.76 \times 10^{-10} \text{ N nm/rad}^{-2} \\ = 0.876 \text{ nN nm rad}^{-2}$$

$$k_\tau = 40 \text{ kcal mole}^{-1} \text{ rad}^{-2} = 2.78 \times 10^{-10} \text{ N nm/rad}^{-2} \\ = 0.278 \text{ nN nm rad}^{-2}$$

Substituting the above values in Eq. (2) and setting $\ell = 0.1421$ nm, we obtain the input parameters for the beam elements

$$d = 0.147 \text{ nm} \\ E_b = 5488 \text{ nN/nm}^2 = 5488 \text{ GPa} \\ G_b = 870.7 \text{ nN/nm}^2 = 870.7 \text{ GPa} \quad (3)$$

The cross-sectional area and moments of inertia are derived from the bond diameter

$$A_b = \frac{\pi d^2}{4} = 0.01688 \text{ nm}^2 \\ I_b = \frac{\pi d^4}{64} = 2.269 \times 10^{-5} \text{ nm}^4 \\ J_b = \frac{\pi d^4}{32} = 4.537 \times 10^{-5} \text{ nm}^4 \quad (4)$$

However, since the modeling of the bond is done using beam elements, it is clear that the results of the analyses would be the same as long as the rigidities $E_b A_b$, $E_b I_b$, $G_b J_b$ of the bond are the same. The constant values of the rigidities arise directly from Eq. (1)

$$E_b A_b = 92.65 \text{ nN} \\ E_b I_b = 0.1245 \text{ nN nm}^2 \\ G_b J_b = 0.0395 \text{ nN nm}^2 \quad (5)$$

It should be noted here that in the model described above one can use a non-linear relationship for the interatomic potential for the carbon-atoms. This has been done successfully by the authors to examine the tensile behavior of nanotubes and nanotube-reinforced composites using the modified Morse interatomic potential. The only difference is that the rigidities of Eq. (5) are not constant but depend on the strain. The resulting rigidities of the equivalent beams are also strain dependent. It has been shown in [11] that the results of the current work provide a good approximation for small strains.

2.1.1. Loading conditions

Since the nanotube possess a linear behavior, to derive the rigidities it is sufficient to apply in the FE model an arbitrary displacement such as to load the nanotube in tension, bending and torsion. The boundary and loading conditions for each case are depicted in Fig. 1.

To simulate tension, an axial displacement u_x was applied at one nanotube’s end having the other end fixed. According to mechanics of materials, the axial reaction force F_x at the support is related to u_x by

$$u_x = \frac{F_x}{E_{eq}A_{eq}}L_n \tag{6}$$

where L_n is the nanotube length. The tensile rigidity is simply obtained from Eq. (6) as

$$(EA)_{eq} = \frac{F_x L_n}{u_x} \tag{7}$$

Similarly, to simulate bending, a transverse displacement u_y was applied at one nanotube’s end having the other end fixed. The transverse force F_y at the support is given by

$$u_y = \frac{F_y}{3E_{eq}I_{eq}}L_n^3 \tag{8}$$

The bending rigidity is simply obtained from Eq. (8) as

$$(EI)_{eq} = \frac{F_y L_n^3}{3u_y} \tag{9}$$

To simulate torsion, a tangential force F_ϕ was applied at one nanotube’s end having the other end fixed. The twist angle ϕ of the loaded end is related to the resulted torque $T = F_\phi R_n$ by

$$\phi = \frac{TL_n}{G_{eq}J_{eq}} \tag{10}$$

where R_n is the nanotube radius. The torsional rigidity is simply obtained from Eq. (10) as

$$(GJ)_{eq} = \frac{TL_n}{\phi} = \frac{F_\phi R_n L_n}{\phi} \tag{11}$$

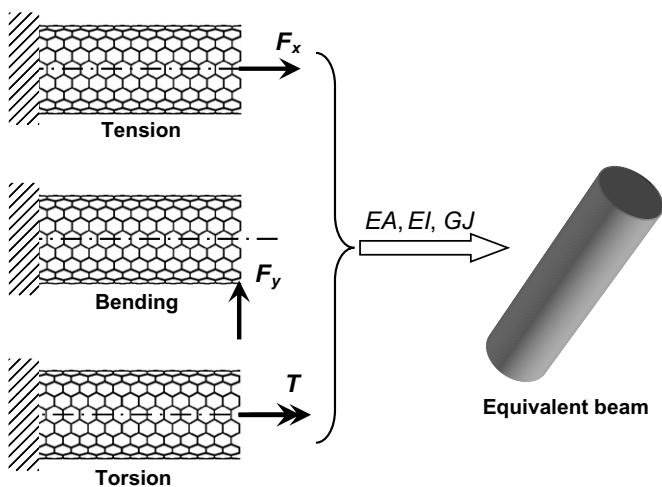


Fig. 1. The concept of the equivalent beam.

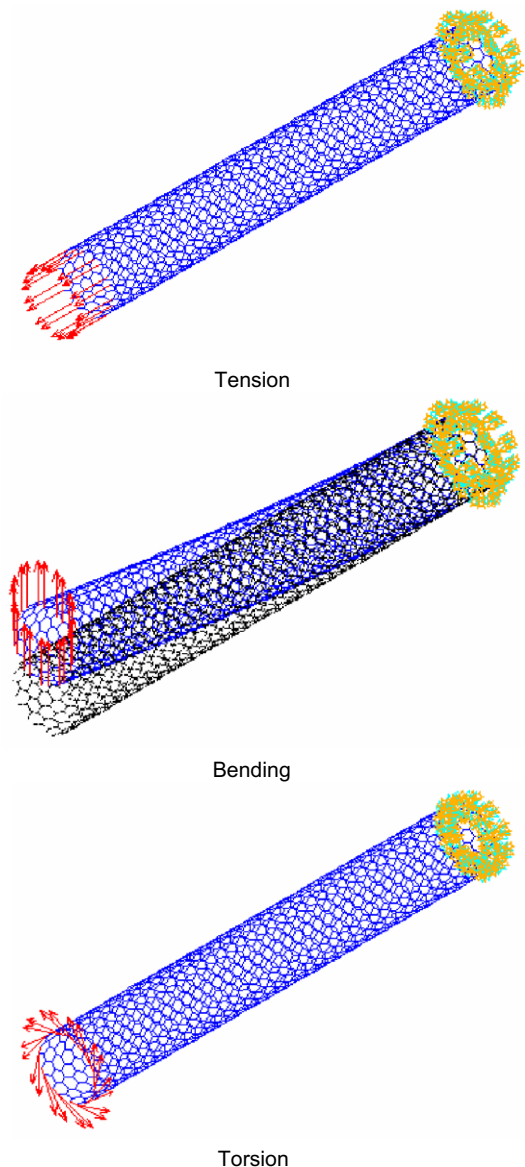


Fig. 2. FE mesh, boundary conditions and deformed shapes for the (10,10) nanotube.

The resulted reaction forces F_x and F_y as well as the angle φ are taken from the FE analysis. Fig. 2 shows the FE mesh, boundary conditions and deformed shapes for the (10,10) nanotube for the three loading cases.

2.1.2. Effect of nanotube length

The usual CNTs manufactured nowadays have very large length (in the order of 1 μm) compared to their diameter (0.5–3 nm). Modeling of the nanotube retaining its actual length would be very time consuming, especially if one wants to study different nanotube types. For example, the FE modeling of a (10,10) nanotube with length 1 μm requires almost 240,000 beam elements. However, modeling of the actual nanotube length is not necessary since the behavior of the nanotubes is length-independent except for very small lengths. The selection of minimum modeling length at which the rigidities stabilize is performed from various analyses conducted with different lengths. Such a parametric study was also conducted here in order to select the minimum modeling length of the equivalent beams. It was selected to model armchair and zigzag nanotubes with chiral indices $n = 5, 10, 15, 20$.

Fig. 3a and b shows the rigidities computed using Eqs. (7), (9) and (11) as functions of nanotube length for the

(20,20) and (20,0) nanotubes, respectively. Variation is observed only at small values of L_n owing to the effect of boundary conditions at the supports. Specifically for bending, the very small initial value is due to the inapplicability of bending theory at small values of nanotube length to diameter ratio. From a certain value of L_n ranging from 40 to 50 nm, all three rigidities stabilize. The same was observed for all other types of nanotubes modelled. Results also show that the rigidities of zigzag nanotubes are smaller than the ones of armchair nanotubes and stabilize at smaller values of L_n . Moreover, it is observed that for both nanotube types bending and torsional rigidities are comparable. The stabilized rigidities' values will be used in the forthcoming sections for evaluation of the equivalent beams.

2.2. Evaluation of the equivalent properties

Evaluation of the elastic properties E_{eq} , G_{eq} and v_{eq} geometrical characteristics A_{eq} , I_{eq} , J_{eq} of the equivalent beam requires the values of the rigidities evaluated using the FE method. However, in order to provide simple relations for the equivalent beam characteristics, it was decided to fit the FE results to simple expressions. This was supported by the values of the rigidities obtained, which seem to relate directly to the chiral index of the nanotubes. In Fig. 4a,

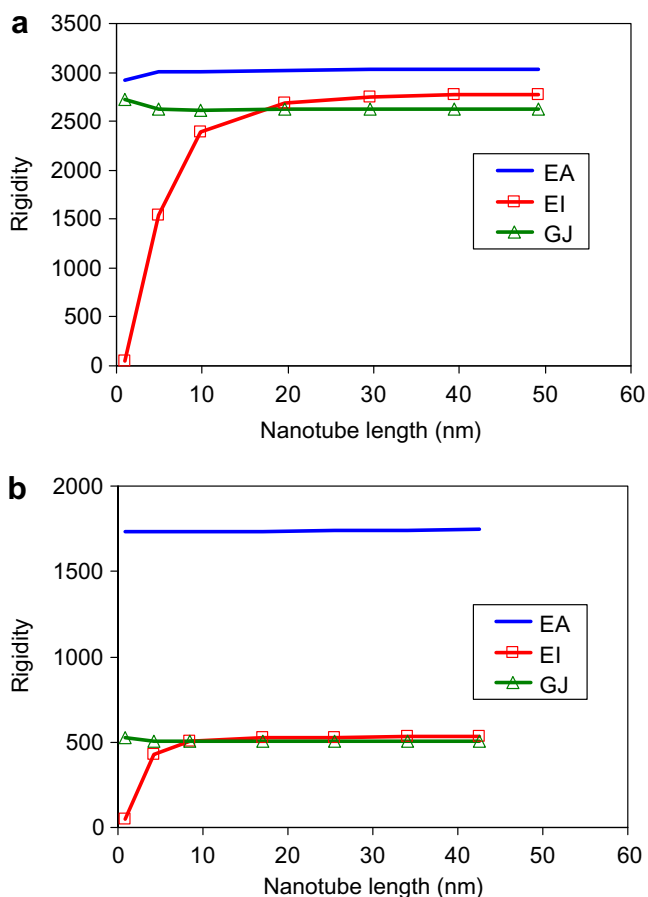


Fig. 3. Variation of rigidities as functions of nanotube length: (a) (20,20) nanotube, (b) (20,0) nanotube.

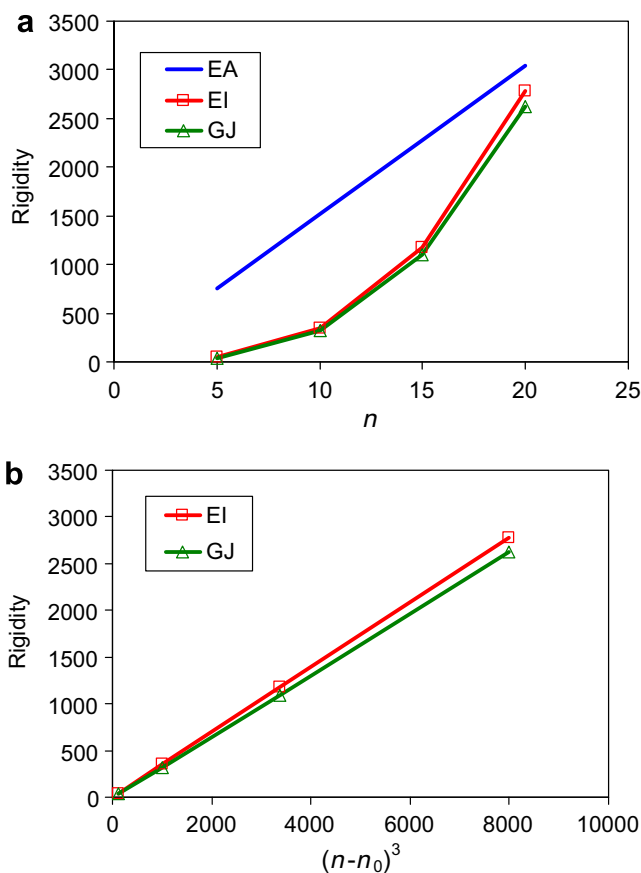


Fig. 4. Variation of rigidities as functions of (a) n and (b) $(n - n_0)^3$: armchair nanotubes.

the stabilized rigidities' values of the armchair nanotubes are presented as functions of chiral index n . It is clear that the tensile rigidity is analogous to n . The bending and torsional rigidities are analogous to the cubic power of n , as shown in Fig. 4b. The same dependences are also obtained for the zigzag nanotubes as shown in Fig. 5. Therefore, we can accurately approximate the rigidities from the following relations (subscript eq refers to the equivalent beam).

$$(EA)_{eq} = \alpha(n - n_0) \tag{12}$$

$$(EI)_{eq} = \beta(n - n_0)^3 \tag{13}$$

$$(GJ)_{eq} = \gamma(n - n_0)^3 \tag{14}$$

The parameters α , β , γ and n_0 are given in Table 1.

The accuracy of the expressions (12)–(14) in fitting the FE results depends on the range of values used for the chiral index n . The range selected in this work ($n = 5–20$) represents the majority of the nanotubes used for analysis or experiments in the literature. For the tensile rigidity the maximum difference between the expression (12) and the FE results is 0.7% for zigzag nanotubes and $n = 5$. This small difference is due to the linear dependency of $(EA)_{eq}$ to n . For the bending and torsional rigidities the maximum differences for zigzag nanotubes ($n = 5$) are 4.8% and 5.2%,

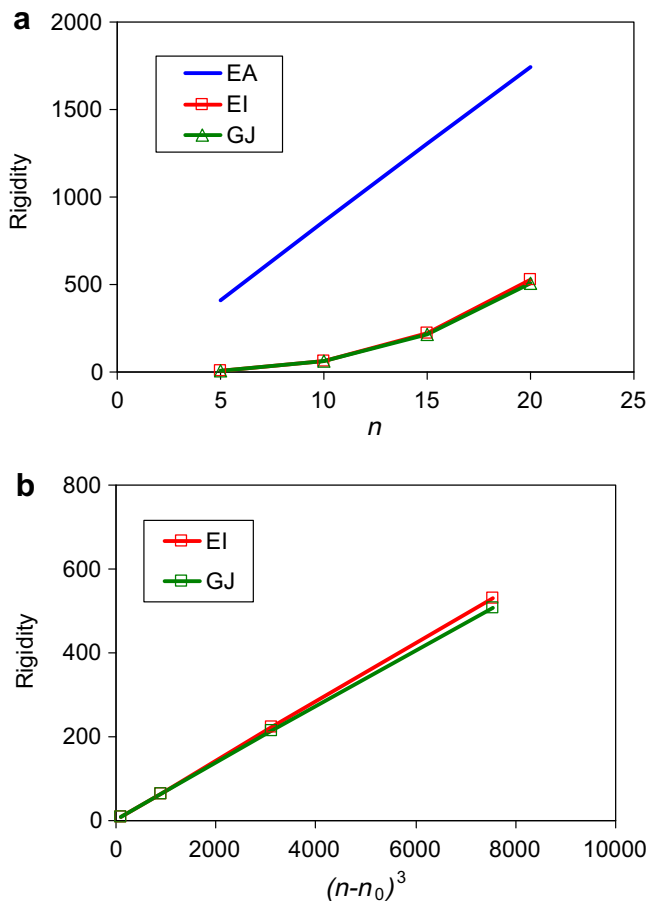


Fig. 5. Variation of rigidities as functions of (a) n and (b) $(n - n_0)^3$: zigzag nanotubes.

Table 1
Values of parameters α , β , γ , n_0

| Parameter | Armchair | Zigzag |
|--------------------------------|----------|--------|
| α (nN) | 151.8 | 89.04 |
| β (nN nm ²) | 0.3469 | 0.0701 |
| γ (nN nm ²) | 0.3284 | 0.0668 |
| n_0 (-) | 0 | 0.381 |

respectively. The larger deviations are due to the cubic power of n and become less than 1% for $n = 10$. It should be noted that, for a specific nanotube, one could use directly the values obtained from the FE analysis and, thus, minimize the error. The accuracy of the FE models, as compared to the literature results, is discussed in Section 3.1.

After establishing the relations between the rigidities and n , the next step is to select the profile of the equivalent beam. Obviously, due to the circular shape of the nanotube's cross-sectional area, circular profiles are more suitable. Thus, we select the solid and hollow cylindrical profiles schematically represented in Fig. 6.

2.2.1. Solid cylinder

Consider an equivalent solid cylinder with diameter D_{eq} . Its diameter, secondary and polar moments of inertia are given by the following relations:

$$A_{eq} = \frac{\pi}{4} D_{eq}^2 \tag{15}$$

$$I_{eq} = \frac{\pi}{64} D_{eq}^4 \tag{16}$$

$$J_{eq} = \frac{\pi}{32} D_{eq}^4 \tag{17}$$

Combining Eqs. (12) and (13) with Eqs. (15) and (16) D_{eq} is derived as follows:

$$\frac{(EI)_{eq}}{(EA)_{eq}} = \frac{1}{16} D_{eq}^2 = \frac{\beta}{\alpha} (n - n_0)^2 \Rightarrow D_{eq} = 4 \sqrt{\frac{\beta}{\alpha}} (n - n_0) \tag{18}$$

Substituting Eq. (18) in Eqs. (15)–(17) the geometrical constants of the equivalent beam are derived as functions of the parameters α , β and γ .

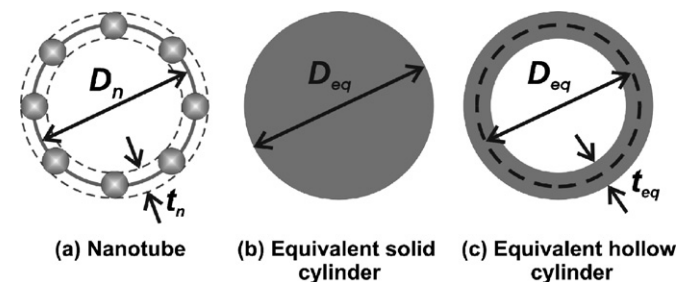


Fig. 6. Schematic representations of the beam profiles.

$$A_{\text{eq}} = \frac{\pi}{4} D_{\text{eq}}^2 = 4\pi \frac{\beta}{\alpha} (n - n_0)^2 \quad (19)$$

$$I_{\text{eq}} = \frac{\pi}{64} D_{\text{eq}}^4 = 4\pi \left(\frac{\beta}{\alpha}\right)^2 (n - n_0)^4 \quad (20)$$

$$J_{\text{eq}} = 2I_{\text{eq}} = 8\pi \left(\frac{\beta}{\alpha}\right)^2 (n - n_0)^4 \quad (21)$$

Now, using Eqs. (12) and (14) we evaluate the elastic moduli of the equivalent beam as

$$E_{\text{eq}} = \frac{(EA)_{\text{eq}}}{A_{\text{eq}}} = \frac{\alpha^2}{4\pi\beta} (n - n_0)^{-1} \quad (22)$$

$$G_{\text{eq}} = \frac{(GJ)_{\text{eq}}}{J_{\text{eq}}} = \frac{\alpha^2\gamma}{8\pi\beta^2} (n - n_0)^{-1} \quad (23)$$

In the case of 3D modeling of the beam, the Poisson ratio is also needed

$$G_{\text{eq}} = \frac{E_{\text{eq}}}{2(1 + \nu_{\text{eq}})} \Rightarrow \nu_{\text{eq}} = \frac{E_{\text{eq}}}{2G_{\text{eq}}} - 1 = \frac{\beta}{\gamma} - 1 \quad (24)$$

Eqs. (19)–(24) fully define the equivalent solid cylinder.

2.2.2. Hollow cylinder

Consider an equivalent hollow cylinder with mean diameter D_{eq} and thickness t_{eq} . Its diameter, secondary moment of inertia and polar moment of inertia are given by the following relations:

$$A_{\text{eq}} = \frac{\pi}{4} [(D_{\text{eq}} + t_{\text{eq}})^2 - (D_{\text{eq}} - t_{\text{eq}})^2] = \pi D_{\text{eq}} t_{\text{eq}} \quad (25)$$

$$I_{\text{eq}} = \frac{\pi}{64} [(D_{\text{eq}} + t_{\text{eq}})^4 - (D_{\text{eq}} - t_{\text{eq}})^4] \quad (26)$$

$$J_{\text{eq}} = \frac{\pi}{32} [(D_{\text{eq}} + t_{\text{eq}})^4 - (D_{\text{eq}} - t_{\text{eq}})^4] \quad (27)$$

In the present case, there are three available equations namely, Eqs. (12)–(14) and four unknown quantities namely, E_{eq} , G_{eq} , D_{eq} and t_{eq} . Therefore, we cannot derive D_{eq} and t_{eq} independently. To overcome this obstacle, we set the nanotube thickness equal to 0.34 nm, which is the commonly adopted value in the literature [7]. Supposing $t_{\text{eq}} = t_n$ and using Eqs. (12), (13) and (25), (26) D_{eq} is derived as

$$\begin{aligned} \frac{(EI)_{\text{eq}}}{(EA)_{\text{eq}}} &= \frac{1}{8} (D_{\text{eq}}^2 + t_n^2) = \frac{\beta}{\alpha} (n - n_0)^2 \Rightarrow D_{\text{eq}} \\ &= \sqrt{8 \frac{\beta}{\alpha} (n - n_0)^2 - t_n^2} \end{aligned} \quad (28)$$

Substituting Eq. (28) in Eqs. (25)–(27) we derive the geometrical constants of the equivalent beam as functions of the parameters α , β and γ .

$$A_{\text{eq}} = \pi D_{\text{eq}} t_n = \pi t_n \sqrt{8 \frac{\beta}{\alpha} (n - n_0)^2 - t_n^2} \quad (29)$$

$$I_{\text{eq}} = \pi t_n \frac{\beta}{\alpha} (n - n_0)^2 \sqrt{8 \frac{\beta}{\alpha} (n - n_0)^2 - t_n^2} \quad (30)$$

$$J_{\text{eq}} = 2\pi t_n \frac{\beta}{\alpha} (n - n_0)^2 \sqrt{8 \frac{\beta}{\alpha} (n - n_0)^2 - t_n^2} \quad (31)$$

Now, using Eqs. (12) and (14) we evaluate the elastic moduli of the equivalent beam as

$$E_{\text{eq}} = \frac{\alpha(n - n_0)}{\pi t_n \sqrt{8 \frac{\beta}{\alpha} (n - n_0)^2 - t_n^2}} \quad (32)$$

$$G_{\text{eq}} = \frac{\alpha\gamma(n - n_0)}{2\pi t_n \beta \sqrt{8 \frac{\beta}{\alpha} (n - n_0)^2 - t_n^2}} \quad (33)$$

and subsequently, the Poisson ratio

$$G_{\text{eq}} = \frac{E_{\text{eq}}}{2(1 + \nu_{\text{eq}})} \Rightarrow \nu_{\text{eq}} = \frac{E_{\text{eq}}}{2G_{\text{eq}}} - 1 = \frac{\beta}{\gamma} - 1 \quad (34)$$

which is the same as Eq. (24). Eqs. (29)–(34) fully define the equivalent hollow cylinder.

From Eq. (34) we observe that the Poisson ratio does not depend on n . For the armchair nanotubes, ν_{eq} equals to 0.049 for both solid and hollow cylinders while for the zigzag ones equals to 0.056.

The computed rigidities, material properties and geometrical characteristics can be also used as a base for modeling more complicated nanotube shapes. Characteristic examples are the cases where CNTs are being used as structural elements to construct high-ordered structures such as super-CNTs and 2D and 3D lattice structures. For all these structures the expressions (12)–(14) can be used instead of Eq. (1) in order to model them as space-frame structures using FE analysis. This is the subject of an ongoing research by the authors.

3. Numerical results

In this section, we compare the suitability of the solid and hollow cylinders in serving as equivalent beams and examine the differences between the dimensions of the equivalent beams and actual nanotube dimensions. The actual diameter of CNTs is given by

$$D_n + t_n = \frac{3L}{\pi} n + 0.34 = 0.1357 \cdot n + 0.34 \quad (\text{armchair nanotubes}) \quad (35)$$

$$D_n + t_n = \frac{\sqrt{3}L}{\pi} n + 0.34 = 0.0783 \cdot n + 0.34 \quad (\text{zigzag nanotubes}) \quad (36)$$

It is very important for the dimensions of the equivalent beam to approximate the actual dimensions of the nanotube. This is more evident in the modeling of CNT-reinforced composites subjected to bending where the accurate computation of the interfacial shear stresses

requires the same outer diameter. Fig. 7 compares the diameters of the equivalent beams (D_{eq} for the solid cylinder and $D_{eq} + t_{eq}$ for the hollow cylinder) with the actual external diameter of the nanotubes. For armchair nanotubes, the diameter of the equivalent hollow cylinder is much closer to the actual nanotube diameter. For zigzag nanotubes, both equivalent shapes differ the same amount from the actual external diameter for $n < 10$, whereas the hollow cylinder is better suited for larger values of the chiral index. We can conclude that in general, the hollow cylinder is more suitable for use as equivalent beam than the solid cylinder.

Fig. 8 shows the variation of elastic moduli with regard to chiral index n . The similar trend of variation obtained for both elastic moduli is due to their direct relation with the Poisson ratio, which is constant and almost equal for both nanotube types. With increasing n , the elastic moduli are significantly reduced, owing to the increase of the nanotube diameter (see Fig. 7), and converge to the values established in the literature, namely 1 TPa for the axial modulus and 0.5 TPa for the shear modulus. Thus, we can conclude that for nanotubes with $n \geq 10$ the established values of the elastic moduli can be used while for

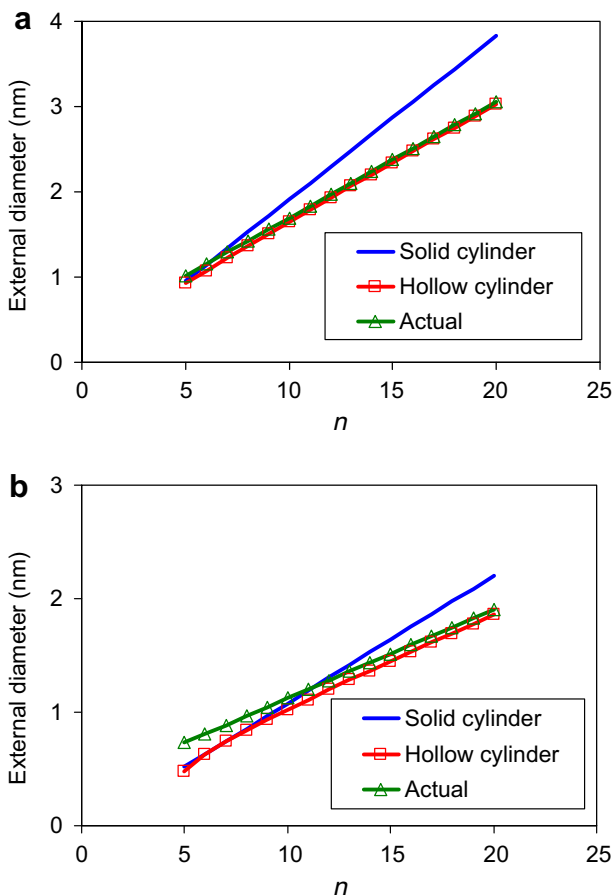


Fig. 7. External diameters as functions of n : (a) armchair nanotubes, (b) zigzag nanotubes.

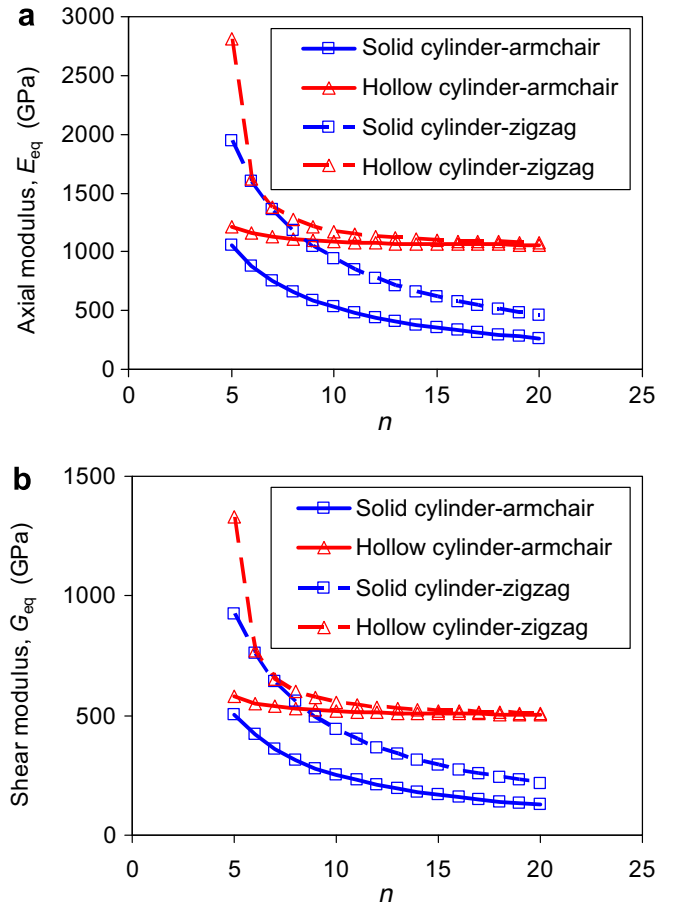


Fig. 8. Variation of (a) E_{eq} and (b) G_{eq} as functions of n .

$n \leq 10$ the elastic moduli of the equivalent beam must be evaluated using the methodology proposed here.

3.1. Comparison with results from the literature

The linear relation between the elastic rigidity and n obtained here (Eq. (12)) has not been reported in the literature. However, a careful examination of the published results verifies this finding. Chang and Gao [12] found using molecular dynamics the following relation for the axial elastic modulus of lengthy nanotubes

$$E = \frac{1}{t_n} \cdot \frac{4\sqrt{3}K}{3\lambda KL_n^2/C + 9} \quad (37)$$

where $K = 742 \text{ nN nm}$ and $C = 1.42 \text{ nN nm}$, and

$$\lambda = \frac{7 - \cos(\pi/n)}{34 + 2 \cos(\pi/n)} \text{ for armchair and}$$

$$\lambda = \frac{5 - 3 \cos(\pi/n)}{14 - 2 \cos(\pi/n)} \text{ for zigzag nanotubes.}$$

Eq. (37) can be rewritten in the form

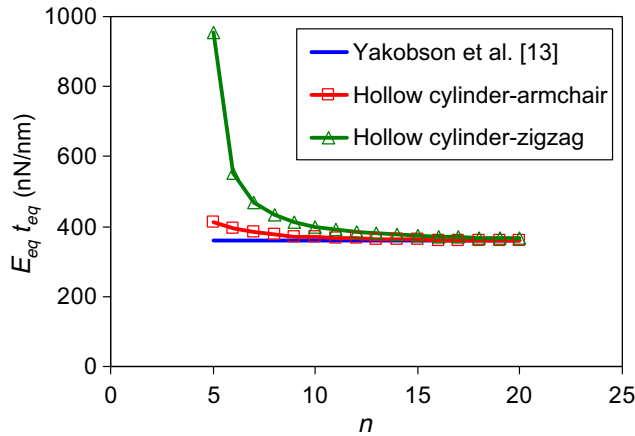


Fig. 9. Variation of $E_{eq}t_{eq}$ as a function of n .

$$EA = \frac{1}{t_n} \cdot \frac{4\sqrt{3}K}{3\lambda KL^2/C + 9} \quad A = \frac{1}{t_n} \cdot \frac{4\sqrt{3}K}{3\lambda KL^2/C + 9} \pi D_n t_n$$

$$\Rightarrow EA = \frac{4\sqrt{3}K}{3\lambda KL^2/C + 9} \pi D_n \quad (38)$$

Using $D_n = \frac{3L}{\pi}n$ for the armchair and $D_n = \frac{L\sqrt{3}}{\pi}n$ for zigzag nanotubes, Eq. (38) is very well fitted to the following expressions (due to the small variation of λ)

$$EA = 154 \cdot n \quad (\text{armchair})$$

$$EA = 89.82 \cdot n \quad (\text{zigzag}) \quad (39)$$

The corresponding relations obtained in this work are found using from Eq. (12) and substituting the parameters of Table 1

$$EA_{eq} = 151.8 \cdot n \quad (\text{armchair})$$

$$EA_{eq} = 89.04 \cdot (n - 0.381) \quad (\text{zigzag}) \quad (40)$$

Eqs. (39) and (40) agree very well especially for larger values of n .

Some researchers have considered the product Et to be steady. For example Yakobson et al. [13] used the value of 360 nN/nm. Fig. 9 compares the present results with the results of Ref. [13]. As can be seen, the assumed invariability of Et is realistic only for large values of n . For $n \leq 10$, the present results significantly deviate from that assumption especially for zigzag nanotubes.

Regarding the shear modulus of CNTs, Tserpes and Papanikos [7] reported a range between 0.381 and 0.485 TPa for the armchair nanotubes and between 0.283

and 0.487 for the zigzag ones (n ranges from 5 and 15). In the present study, dividing Eq. (14) with the nanotube's polar moment of inertia $J_n = \frac{\pi}{32} [(D_n + t_n)^4 - (D_n - t_n)^4]$, we get the range 0.39–0.48 TPa for the armchair and 0.23–0.46 TPa for the zigzag nanotubes, which correlate very well with the published values.

4. Conclusions

Presented in this paper is a methodology for the evaluation of the elastic moduli and geometrical characteristics of beams that possess the same mechanical behavior with CNTs. Approximate relations between the equivalent properties and chiral index were proposed for armchair and zigzag nanotubes. The accuracy of the proposed relations in predicting the elastic moduli of CNTs was verified through comparison with relative results published in the literature. It is concluded that:

- The rigidities of the nanotubes can be directly related to chiral index n .
- The equivalent hollow cylinder simulates better the mechanical behavior of CNTs.
- The equivalent elastic moduli of nanotubes with small diameters show large variation.

References

- [1] G. Odegard, T. Gates, T. Wise, C. Park, E. Siochic, *Composites Science and Technology* 63 (2003) 1671.
- [2] G. Seidel, D. Lagoudas, *Mechanics of Materials* 38 (2006) 884.
- [3] B. Ashrafi, P. Hubert, *Composites Science and Technology* 66 (2006) 387.
- [4] A. Haque, A. Ramasetty, *Composite Structures* 71 (1) (2005) 68.
- [5] Y. Liu, X. Chen, *Mechanics of Materials* 35 (2003) 69.
- [6] X. Chen, Y. Liu, *Computational Materials Science* 29 (2004) 1.
- [7] K.I. Tserpes, P. Papanikos, *Composites Part B* 36 (2005) 468.
- [8] G. Odegard, T. Gates, L. Nicholson, K. Wise, *Composites Science and Technology* 62 (2002) 1869.
- [9] W. Cornell, P. Cieplak, C. Bayly, et al., *Journal of American Chemical Society* 117 (1995) 5179.
- [10] W. Jorgensen, D. Severance, *Journal of American Chemical Society* 112 (1990) 4768.
- [11] K.I. Tserpes, P. Papanikos, G. Labeas, Sp. Pantelakis, *Theoretical and Applied Fracture Mechanics* 49 (2008) 51.
- [12] T. Chang, H. Gao, *Journal of the Mechanics and Physics of Solids* 51 (2003) 1059.
- [13] B. Yakobson, C. Brabec, J. Bernholc, *Physical Review Letters* 76 (14) (1996) 2511.